

# JWST transmission spectroscopy of HD 209458b: a super-solar metallicity, a very low C/O, and no evidence of CH<sub>4</sub>, HCN, or C<sub>2</sub>H<sub>2</sub>

QIAO XUE <sup>1,2</sup> JACOB L. BEAN <sup>1</sup> MICHAEL ZHANG <sup>1</sup> LUIS WELBANKS <sup>3</sup> JONATHAN LUNINE,<sup>4</sup>  
AND PRUNE AUGUST <sup>1</sup>

<sup>1</sup>*Department of Astronomy & Astrophysics, University of Chicago, Chicago, IL, USA*

<sup>2</sup>*School of Physics and Astronomy, Shanghai Jiaotong University, Shanghai, CN*

<sup>3</sup>*School of Earth & Space Exploration, Arizona State University, Tempe, AZ 85287, USA*

<sup>4</sup>*Department of Astronomy, Cornell University, Ithaca, NY, USA*

## ABSTRACT

We present the transmission spectrum of the original transiting hot Jupiter HD 209458b from 2.3 – 5.1  $\mu\text{m}$  as observed with the NIRC*am* instrument on the James Webb Space Telescope (JWST). Previous studies of HD 209458b’s atmosphere have given conflicting results on the abundance of H<sub>2</sub>O and the presence of carbon- and nitrogen-bearing species, which have significant ramifications on the inferences of the planet’s metallicity (M/H) and carbon-to-oxygen (C/O) ratio. We detect strong features of H<sub>2</sub>O and CO<sub>2</sub> in the JWST transmission spectrum, which when interpreted using a retrieval that assumes thermochemical equilibrium and fractional grey cloud opacity yields  $3_{-1}^{+4} \times$  solar metallicity and  $\text{C/O} = 0.11_{-0.06}^{+0.12}$ . The derived metallicity is consistent with the atmospheric metallicity-planet mass trend observed in solar gas giants. The low C/O ratio suggests that this planet has undergone significant contamination by evaporating planetesimals while migrating inward. We are also able to place upper limits on the abundances of CH<sub>4</sub>, C<sub>2</sub>H<sub>2</sub> and HCN of  $\log(\chi_{\text{CH}_4}) = -5.6$ ,  $\log(\chi_{\text{C}_2\text{H}_2}) = -5.7$ , and  $\log(\chi_{\text{HCN}}) = -5.1$ , which are in tension with the recent claim of a detection of these species using ground-based cross-correlation spectroscopy. We find that HD 209458b has a weaker CO<sub>2</sub> feature size than WASP-39b when comparing their scale-height-normalized transmission spectra. On the other hand, the size of HD 209458b’s H<sub>2</sub>O feature is stronger, thus reinforcing the low C/O inference.

*Keywords:* Exoplanet atmospheres (487), Exoplanet atmospheric composition (2021), Transmission spectroscopy (2133)

## 1. INTRODUCTION

Detected initially by the radial velocity method in 1999, the hot Jupiter HD 209458b was the first exoplanet found to transit its host star (Charbonneau et al. 2000; Henry et al. 2000). Since then, it has been one of the most frequently studied exoplanets and it has been

the subject of a number of breakthroughs that sparked the study of exoplanetary atmospheres. Via transmission spectroscopy, it was the subject of the first exoplanet atmosphere detection (Charbonneau et al. 2002), the first found to have an escaping atmosphere (Vidal-Madjar et al. 2003), the first observed to possess atomic

carbon and oxygen (Vidal-Madjar et al. 2004), and the first to have its orbital velocity measured, thus turning the system into a double-lined spectroscopic binary (Snellen et al. 2010). It was one of the first two exoplanets with detected infrared emission (Deming et al. 2005), and it was one of the first two exoplanets with the spectroscopic identification of water (Deming et al. 2013a). What’s more, it was once thought to possess a stratospheric temperature inversion (Knutson et al. 2008; Burrows et al. 2007), although that hypothesis was later refuted by subsequent observations and analysis (Diamond-Lowe et al. 2014; Schwarz et al. 2015; Line et al. 2016).

HD 209458b is still among the best targets for atmospheric study in this era of thousands of known transiting planets. It has a relatively bright host star, a favorable planet-to-star radius ratio, a high equilibrium temperature, and a low surface gravity. Ultimately, it has the highest transmission spectroscopy metric ( $\sim 900^1$ ) of all known exoplanets (Kempton et al. 2018).

Despite its great observability, several fundamental questions about the composition of HD 209458b’s atmosphere remain unsolved. One of these questions is its atmospheric water abundance. Several groups have derived sub-solar water abundances from measurements of its atmosphere (Madhusudhan et al. 2014; MacDonald & Madhusudhan 2017a; Brogi et al. 2017; Welbanks et al. 2019a; Pinhas et al. 2019), with a recent re-analysis providing estimates consistent with solar expectations within the uncertainties (Welbanks & Madhusudhan 2021). This could be caused by an overall low metallicity or just a low oxygen abundance in the planet, neither of which are expected by standard models for giant planet formation (Öberg & Bergin 2016; Booth et al.

2017). However, Line et al. (2016), Sing et al. (2016) and Tsiaras et al. (2018) also reported solar to super-solar H<sub>2</sub>O abundances, which is more in line with expectations from traditional planet formation models (Owen & Encrenaz 2006; Öberg et al. 2011).

A second open question surrounds the carbon and nitrogen chemistry. Interpretation of the *Hubble Space Telescope* (*HST*) transmission spectrum initially suggested strong evidence for NH<sub>3</sub> and/or HCN (MacDonald & Madhusudhan 2017a), but a subsequent analysis lowered the detection significance and highlighted NH<sub>3</sub> as being the more likely of the two (MacDonald & Madhusudhan 2017b). On the other hand, two high-resolution spectroscopy (HRS) analyses both claimed the presence of HCN (Hawker et al. 2018; Giacobbe et al. 2021). The latter of these two studies also claimed the detection of NH<sub>3</sub>, CH<sub>4</sub>, and C<sub>2</sub>H<sub>2</sub> in addition to H<sub>2</sub>O and CO (Giacobbe et al. 2021). When assuming equilibrium chemistry and a clear atmosphere, the presence of all of these molecules together suggests a highly sub-solar metallicity (<1% of solar) and/or a C/O ratio of around 1 or higher (compare to the solar value of 0.59, Asplund et al. 2021), which together challenge planet formation models (Mousis et al. 2012; Madhusudhan et al. 2014).

In this paper, we present the first transmission spectrum of the archetypical hot Jupiter HD 209458b obtained with the *James Webb Space Telescope* (*JWST*) to answer these long-standing questions. We describe our observations and data analysis in §2, atmospheric modeling in §3 and results in §4.

## 2. OBSERVATIONS AND DATA ANALYSIS

We observed two transits of HD 209458b with *JWST*’s NIRC*am* instrument (Greene et al. 2017) on November 10 and 16, 2022 (program GTO 1274, J. Lunine PI). Each observation lasted 8.01 hours, which is long enough to sample the 3.12-hour transit and the baseline flux

<sup>1</sup> <https://tess.mit.edu/science/tess-acwg/>

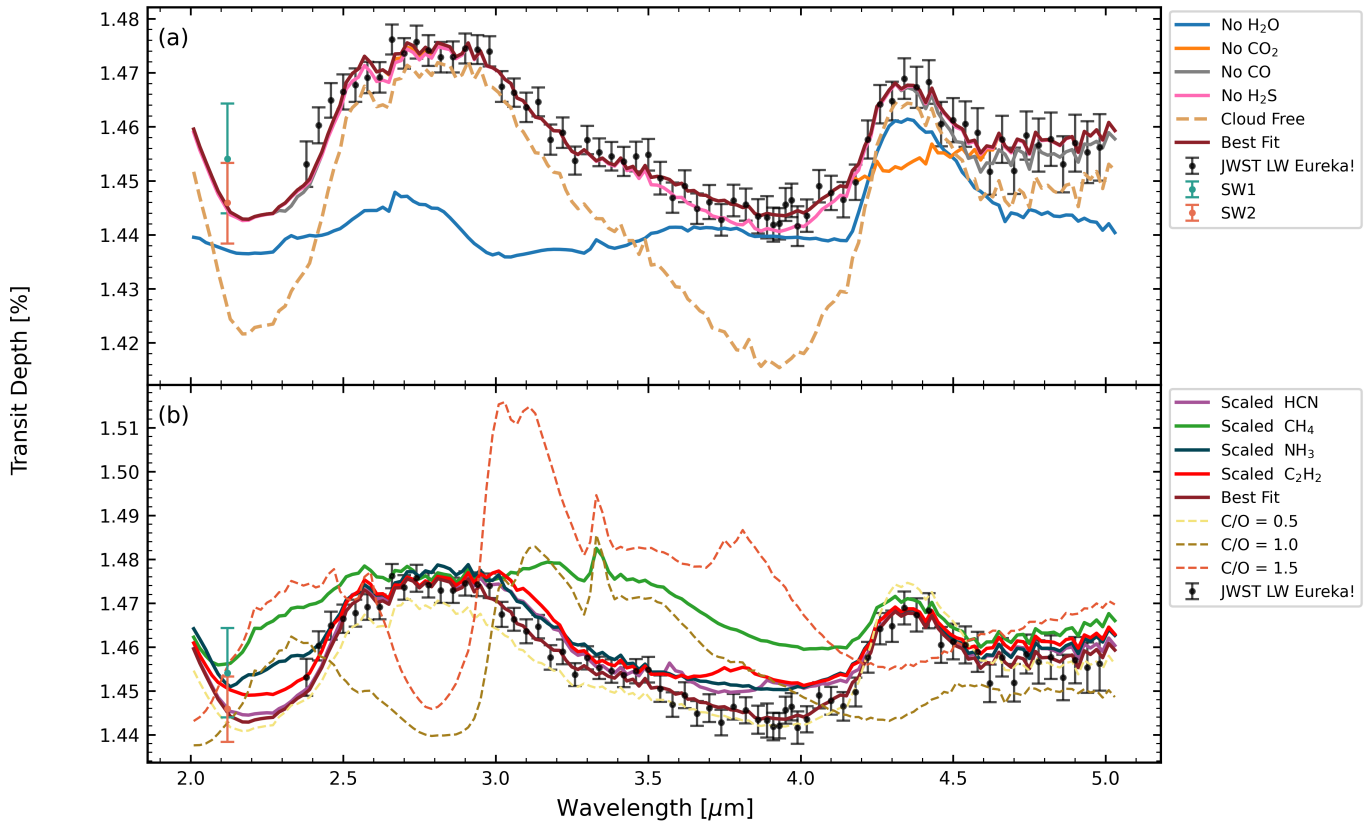


**Figure 1.** (a): JWST NIRCcam data reduced by *Eureka!* (points with error bars). The short-wavelength data at  $2.12 \mu\text{m}$  are plotted but not included in the retrieval. The best-fit chemical equilibrium model is shown as the solid maroon line. Absorption contributed by  $\text{H}_2\text{O}$ ,  $\text{CO}_2$ ,  $\text{CO}$ ,  $\text{H}_2\text{S}$  and cloud are highlighted. (b): Model spectra of HD 209458b when scaling the abundances of  $\text{HCN}$ ,  $\text{CH}_4$ ,  $\text{NH}_3$ ,  $\text{C}_2\text{H}_2$  to artificially higher levels are plotted with solid lines (see §4 for more details). Models with different C/O are plotted with dashed lines. The data behind the figure can be found in §6.

**Table 1.** White light curve best-fit parameters by *Eureka!* and *SPARTA*.

	Visit 1		Visit 2	
	<i>Eureka!</i>	<i>SPARTA</i>	<i>Eureka!</i>	<i>SPARTA</i>
$t_0$ (MJD)	$59889.72649 \pm 0.00003$	$59889.72646 \pm 0.00003$	$59893.25125 \pm 0.00002$	$59893.25120 \pm 0.00003$
$a/R_*$	/	/	$8.84 \pm 0.02$	$8.84 \pm 0.02$
$i$ ( $^\circ$ )	/	/	$86.74 \pm 0.04$	$86.74 \pm 0.03$

before and after the transit. Both observations used the module A grism R mode to obtain time-series near-infrared spectra in the long-wavelength (LW) channel. The first observation collected data with the F444W filter, yielding spectra from  $3.86$  to  $5.06 \mu\text{m}$ . The second obser-

vation used the F322W2 filter, yielding spectra from  $2.36$  to  $4.02 \mu\text{m}$ .

Both visits employed the SUBGRISM64 sub-array and BRIGHT2 readout pattern. The first observation used six groups per integration for a total of 7,107 integrations, while the second

used four groups per integration for a total of 9,473 integrations. Photometry was also obtained simultaneously in the short-wavelength (SW) channel during each LW channel observation. The SW photometry for both visits was obtained in a narrow band at  $2.12\ \mu\text{m}$  using the WLP4 filter with the BRIGHT1 readout pattern.

We reduced and analyzed the LW data independently using two different pipelines. The first pipeline we used is **Eureka!** (Bell et al. 2022), which has been utilized extensively by the *JWST* Transiting Exoplanet Early Release Science (JTEC ERS) Team (JTEC ERS Team et al. 2023; Ahrer et al. 2023; Alderson et al. 2023; Feinstein et al. 2023; Rustamkulov et al. 2023; Coulombe et al. 2023). The second pipeline we used is **SPARTA**<sup>2</sup>, which was first utilized for the MIRI/LRS phase curve of GJ 1214b (Kempton et al. 2023) and is also now being included in the JTEC ERS analyses of MIRI/LRS data of WASP-43b (Bell et al., submitted) and WASP-39b (Powell et al., submitted).

Our **Eureka!** implementation follows the analyses of NIRCcam data presented in Ahrer et al. (2023) and Bean et al. (2023). The first two stages in **Eureka!** are identical with those in the *JWST* Science Calibration Pipeline (`jwst`) except that we did a group-level background subtraction and we increased the jump detection threshold to 6.0. Following Stage 2, **Eureka!** performed a column-by-column linear fit to calculate the background in the region beyond 13 pixels relative to the center of the spectral trace and subtracted it from the region of interest. Correction of the curvature of the spectral trace was performed by shifting columns to align the center of the spectral trace along the same row. Then optimal spectral extraction as defined in Horne (1986) was performed for each integration within eight pixels on both sides of

the trace. The spatial profile used in the optimal extraction weighting is based on a median frame cleared of  $10\sigma$  outliers. We excluded the five spectroscopic light curves with scattering factors greater than  $1.6\times$  photon noise in the presented spectra.

**SPARTA** is a new, end-to-end pipeline that begins with the raw, uncalibrated files with *JWST*. **SPARTA** has its own up-the-ramp fitting that does not depend on the *JWST* pipeline. The detailed reduction algorithms of **SPARTA** can be found in Kempton et al. (2023). For F332W2 and F444W, we let the spectral center be at the 35th and 33rd pixel respectively and the extraction window to be 8 pixels. For spectroscopic light curve fitting, we excluded three data points with scattering factors greater than 1.35 or smaller than 1.0. As with **Eureka!**, the transit light curve parameters were estimated using the dynamic nested sampling algorithm (Higson et al. 2018) as implemented by the `dynesty` package<sup>3</sup>.

We generated both “white” light curves that were summed over the full bandpass of each observation and spectroscopic light curves that were summed over  $0.04\ \mu\text{m}$  each (yielding 69 channels in total) for the LW data. A  $9\sigma$  outlier rejection on each light curve were performed and we fit each light curve with a transit model from the `batman` code (Kreidberg 2015) combined with a systematics model that is linear with time (i.e.,  $c_0 + c_1t$ ). We trimmed the first 990 integrations of the first observation and 1,176 integrations of the second (both approximately the first 1 hour) due to the strong exponential-like ramp at the beginning of the observations.

We adopted the orbital period as 3.52474859 days (Stassun et al. 2017), eccentricity as 0.0, and argument of periapsis as  $90.0^\circ$ . The inclination  $i$  and semi-major axis in units of the host star radius  $a/R_s$  were de-

<sup>2</sup> <https://github.com/ideasrule/sparta>

<sup>3</sup> <https://dynesty.readthedocs.io/en/stable/>

terminated by fitting the white light curve of the second visit because it has less noise than the first visit (more photons were collected in these shorter wavelength data). Then  $i$  and  $a/R_s$  were fixed in the analysis of all the spectroscopic channels. The mid-transit time of the two observations is determined by fitting the white light curve of each observation. The best estimated parameters can be found in Table 1.

As is typical, the measured transit depths depend on the limb darkening assumptions. We tried using limb-darkening coefficients for a four-parameter “non-linear” law calculated from 3D stellar model atmospheres specific to HD 209458 (Hayek et al. 2012), but the results do not match our data well. Therefore, we elected to instead fit for the limb darkening coefficients in the light curve modeling. We adopted the quadratic limb-darkening law reparameterised by Kipping (2013).

The SW data were reduced by enabling photometric analysis in *Eureka!* (see Bean et al. 2023). First, the centroid of the image was determined by a 2D Gaussian fit. We then performed aperture photometry with radius of 45 pixels and a background annulus spanning from 100 to 120 pixels because this combination minimized the scatter in the light curve. We didn’t correct for  $1/f$  noise because it was not evident in our data. As we did for the LW data, the light curves from SW were fitted using dynamic nested sampling.

The transmission spectrum of HD 209458b measured in the LW and SW NIRCcam data by *Eureka!* is shown in Figure 1. The weighted mean difference between the independent *Eureka!* and SPARTA reductions of the LW data is  $1.67 \sigma$  (see Figure 6 for the comparison). The overlapping region of the two LW filters (3.90 to 4.00  $\mu m$ ) agrees at  $1.9 \sigma$  for *Eureka!* reduction and  $0.37 \sigma$  for SPARTA. However, we didn’t include the SW data in the atmospheric retrieval (see next section) because of the high

scatter seen in the light curves ( $\sim 10 \times$  photon noise).

### 3. ATMOSPHERIC MODELING

We retrieved the atmospheric properties of HD 209458b by fitting the *JWST* spectrum using PLATON<sup>4</sup> (Zhang et al. 2019, 2020), which has been used to determine the properties of several hot Jupiters (Jiang et al. 2021; Ahrer et al. 2022; Spyratos et al. 2023; Bean et al. 2023; August et al. 2023). Our retrieval setup assumed an isothermal atmosphere with equilibrium chemistry and a “patchy” grey cloud deck (the latter motivated by Line & Parmentier 2016). The retrieval included the planet radius at  $10^5$  Pa, temperature, metallicity ( $[M/H] = \log(M/H) - \log(M/H)_{\text{Sun}}$ ), carbon-to-oxygen (C/O) ratio, cloud-top pressure, and cloud fraction on the day-nightside terminator as free parameters. For the cloud fraction we use the prescription of Pinhas et al. (2019). Additionally, we included the mixing ratios of CH<sub>4</sub>, NH<sub>3</sub>, C<sub>2</sub>H<sub>2</sub>, and HCN as free parameters (with log-uniform priors from  $10^{-10}$  to  $10^{-2}$ ) to obtain constraints on their abundances separate from the equilibrium chemistry predictions because these four species are key detections in Giacobbe et al. (2021).

Two additional cloud models are tested as follows. The first one is with spectral slope (where the absorption coefficient is characterized by  $\alpha \propto A \times \lambda^{\text{slope}}$ ) (Zhang et al. 2019). Besides the six parameters described above, we retrieved scattering amplitude  $A$  and slope, but neither of them can be well constrained. The second is Mie scattering which has a complex refractive index of  $1.33 - 0.1j$ . We retrieved number density and the size of particles and the resulting C/O and  $[M/H]$  are consistent with the simpler “patchy” grey cloud deck model described above.

<sup>4</sup> <https://platon.readthedocs.io/en/latest/>



The abundance grid is computed by `FastChem`<sup>5</sup> and has five dimensions: species name (in total 34 atomic and molecular species, same as [Zhang et al. \(2019\)](#)), temperature (100 – 3000K with 100K interval), pressure ( $10^{-4}$  –  $10^8$  Pa with decade interval), metallicity (from  $[M/H] = -1$  to  $[M/H] = 2$  with 0.03 interval) and C/O (0.001 to 2.0<sup>6</sup>). The carbon abundance is computed by scaling the solar oxygen abundance with different C/O, and the other elements’ abundances (except H and He) are scaled with metallicity.

The absorption coefficients used in the modeling are from the `DACE` opacity database<sup>7</sup> with a resolution of  $R = 100,000$  over 0.5 – 12  $\mu\text{m}$ . We included  $\text{CH}_4$ ,  $\text{CO}$ ,  $\text{CO}_2$ ,  $\text{H}_2\text{O}$ ,  $\text{H}_2\text{S}$ ,  $\text{NH}_3$ ,  $\text{C}_2\text{H}_2$ ,  $\text{HCN}$ , and  $\text{SO}_2$  as these are the molecules making major contribution within this wavelength range ([Pinhas et al. 2019](#)). The adopted absorption coefficients that are compatible with `PLATON` used in our retrieval can be found in §6.

As a consistency check, we used `PLATON` to retrieve the properties of WASP-39b from the `JTEC ERS NIRSpec G395H` spectrum of the planet ([Alderson et al. 2023](#)). We removed the data from 3.9  $\mu\text{m}$  to 4.1  $\mu\text{m}$  on WASP-39b’s spectrum that covers the  $\text{SO}_2$  absorption feature produced by photochemistry ([Tsai et al. 2023](#)). The best fit has  $T = 982^{+40}_{-39}$  K,  $[M/H] = 1.39 \pm 0.16$  and  $\text{C/O} = 0.66^{+0.11}_{-0.25}$ , which are consistent with the results in [Alderson et al. \(2023\)](#) and [Constantinou et al. \(2023\)](#). However, we found a strong degeneracy between temperature and  $R_p$  (see more discussion of this in the next section).

## 4. RESULTS

<sup>5</sup> <https://github.com/exoclimate/FastChem>

<sup>6</sup> the interval is non-linear: [0.001, 0.005, 0.01, 0.02, 0.03, 0.04, 0.05, 0.1, 0.2, 0.4, 0.5, 0.6, 0.7, 0.8, 0.9, 0.95, 1.0, 1.05, 1.1, 1.2, 1.4, 1.6, 1.8, 2.0]

<sup>7</sup> <https://dace.unige.ch>.

In Figure 1(a) we show the best-fit model to our *JWST* transmission spectrum of HD 209458b, with the contributions from  $\text{H}_2\text{O}$ ,  $\text{CO}_2$ ,  $\text{CO}$ ,  $\text{H}_2\text{S}$  and the patchy cloud highlighted. The absorption features in the spectrum are primarily due to water (feature centered at 2.8  $\mu\text{m}$ ) and carbon dioxide (feature centered at 4.3  $\mu\text{m}$ ), with perhaps a minor contribution from  $\text{H}_2\text{S}$ . The water and carbon dioxide features are reduced in amplitude by about a factor of two due to the presence of a cloud deck. Our data favor a cloud patchiness fraction of  $\sim 68\%$  at  $3.0\sigma$  significance<sup>8</sup>. Previous *HST*/*WFC3* observations taken at shorter wavelengths ([Deming et al. 2013b](#)) identified water vapour. This is the first detection of  $\text{CO}_2$  in HD209458b’s atmosphere, continuing the trend of detections of this molecule using *JWST* after WASP-39b ([JTEC ERS Team et al. 2023](#)), HD 149026b ([Bean et al. 2023](#)), and K2-18b ([Madhusudhan et al. 2023](#)). There is no evidence for additional absorbers.

In Figure 1(b) we present models where we scale our equilibrium abundance of  $\text{CH}_4$ ,  $\text{NH}_3$ ,  $\text{C}_2\text{H}_2$ , and  $\text{HCN}$  to the notional abundances from [Giacobbe et al. \(2021, their Extended Data Table 4\)](#), which gave the maximum cross-correlation signal in their data on a species-by-species basis. These molecules have absorption features in our bandpass and would have shown up (to varying degree) if their abundances were as high as those suggested by [Giacobbe et al. \(2021\)](#). By including the volume mixing ratios of  $\text{CH}_4$ ,  $\text{NH}_3$ ,  $\text{C}_2\text{H}_2$ , and  $\text{HCN}$  as free parameters in our retrieval, we provide  $3\sigma$  upper limits of (see Figure 2)  $\log(\chi_{\text{CH}_4}) = -5.6$ ,  $\log(\chi_{\text{NH}_3}) = -4.2$ ,  $\log(\chi_{\text{C}_2\text{H}_2}) = -5.7$ , and  $\log(\chi_{\text{HCN}}) = -5.1$ . The posteriors for the abundances of all four molecules are consistent with the chemical equilibrium prediction from our best-fit model.

<sup>8</sup> calculated as median divided by deviation

**Table 2.** Equilibrium chemistry retrieval results.

Parameter	<i>HST</i> /WFC3 + <i>JWST</i>	<i>JWST</i> only	<i>JWST</i> only
	(Eureka!)	(Eureka!)	(SPARTA)
$R_p$ ( $R_J^a$ )	$1.339^{+0.007}_{-0.006}$	<b><math>1.353^{+0.006}_{-0.007}</math></b>	$1.350^{+0.006}_{-0.006}$
T (K)	$1290^{+83}_{-81}$	<b><math>1088^{+103}_{-88}</math></b>	$1126^{+85}_{-69}$
[M/H]	$0.69^{+0.34}_{-0.25}$	<b><math>0.54^{+0.30}_{-0.23}</math></b>	$0.86^{+0.33}_{-0.49}$
C/O	$0.23^{+0.12}_{-0.15}$	<b><math>0.11^{+0.02}_{-0.06}</math></b>	$0.06^{+0.10}_{-0.04}$
$\log_{10}(\text{Cloudtop Pressure})$ (Pa)	$1.32^{+0.45}_{-0.44}$	<b><math>1.69^{+0.50}_{-0.68}</math></b>	$1.77^{+0.38}_{-0.62}$
cloud fraction	$0.82^{+0.09}_{-0.09}$	<b><math>0.68^{+0.19}_{-0.20}</math></b>	$0.75^{+0.19}_{-0.28}$
WFC3 offset (ppm)	$126^{+12}_{-11}$	/	/

<sup>a</sup> Assumed Jupiter radius =  $7.1492 \times 10^7$  m

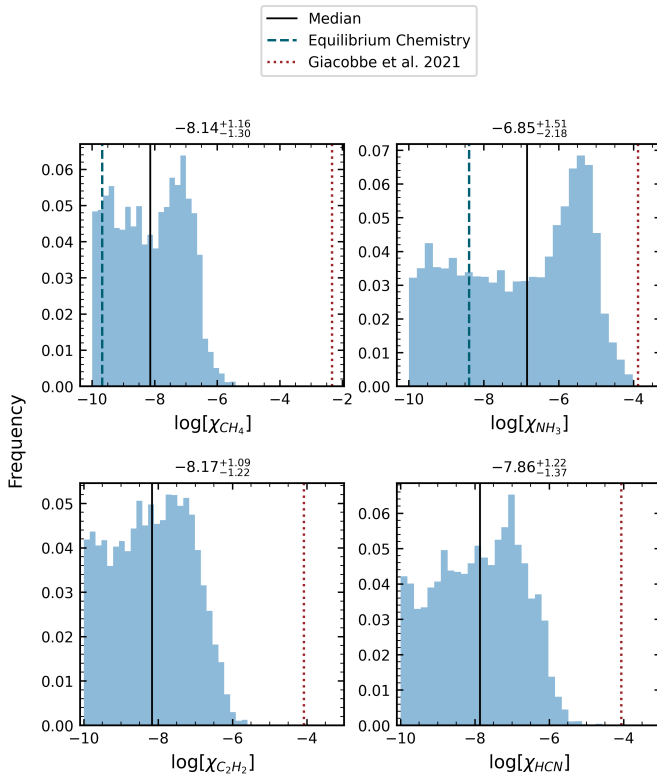


**Figure 2.** Posteriors of the mixing ratios of  $\text{CH}_4$ ,  $\text{NH}_3$ ,  $\text{C}_2\text{H}_2$  and  $\text{HCN}$ . The black lines show the median of the posterior. The blue dashed lines indicate the abundance predicted by equilibrium chemistry at  $T = 1088$  K and  $P = 49$  Pa (0.5 mbar). For  $\text{C}_2\text{H}_2$  and  $\text{HCN}$  the equilibrium values are off the plots to the left. The red dotted lines show the proposed abundances of [Giacobbe et al. \(2021\)](#)

Of the four extra molecules that we explored, only the notional abundance of  $\text{NH}_3$  from [Giacobbe et al. \(2021\)](#) is potentially consistent with our retrieval results i.e., our  $3\sigma$  upper limit is within an order of magnitude of their abundance). Our posterior for  $\text{NH}_3$  is not bounded on the low end, which is consistent with the constraints for this molecule from both [MacDonald & Madhusudhan \(2017a\)](#) and [MacDonald & Madhusudhan \(2017b\)](#), which are based on *HST*/WFC3 data. Therefore, the current space-based data are unable to determine if the molecule is present at equilibrium or higher abundances.

To test if the cloud prescriptions would influence the detection of  $\text{CH}_4$ ,  $\text{NH}_3$ ,  $\text{C}_2\text{H}_2$ , and  $\text{HCN}$ , we repeated the two cloud models described in §3 (paragraph 2) and recomputed the abundances of these four key molecules. We report the constrained  $3\sigma$  upper limits of  $\text{CH}_4$ ,  $\text{C}_2\text{H}_2$ , and  $\text{HCN}$  are all less than  $10^{-5}$ .

The abundances suggested by [Giacobbe et al. \(2021\)](#) for the other three molecules we explored ( $\text{CH}_4$ ,  $\text{HCN}$ , and  $\text{C}_2\text{H}_2$ ) are highly inconsistent with our results (i.e., our  $3\sigma$  upper limits are at least an order of magnitude lower than their abundances). However, the reported volume mixing ratios from [Giacobbe et al. \(2021\)](#) are from models that maximize the cross-correlation functions for each species individually, and thus are not retrieved values

with proper uncertainties. Therefore, the spectra shown in Figure 1(b) might not represent the actual inference from their data, and further analysis is needed to assess the level of agreement.

In Figure 3, we show the corner plot for our chemical equilibrium retrieval on the *Eureka!* reduction. Similar to our retrieval on WASP-39b, we found a strong correlation between the temperature and the planet radius, which we believe is caused by the limitation of wavelength coverage. Specifically, the spectrum lacks the continuum fully outside molecular absorption bands and the multiple bands of the same molecule that are helpful for breaking degeneracies in transmission spectra (Benneke & Seager 2012). On the other hand, these *JWST* data precisely resolve the shape of the H<sub>2</sub>O and CO<sub>2</sub> features, and our assumption of chemical equilibrium provides additional constraints on the retrieval.

To test the robustness of the wavelength coverage of our *JWST* data, we compared it with the best-fit parameters from joint *HST*/WFC3 and *JWST* fitting, and the retrieved [M/H], C/O are consistent at greater than  $0.5\sigma$ . We also conducted a test to see the impact of the minor difference in the spectrum obtained by a different data reduction pipeline. We found the retrieved parameters from *Eureka!*'s spectrum are within  $1\sigma$  of those from SPARTA's spectrum. The best retrieved atmospheric properties can be found in Table 2.

Using only the *JWST* data, PLATON favors a metallicity of  $3_{-1}^{+4} \times \text{solar}$  and a C/O =  $0.11_{-0.06}^{+0.12}$  (bolded column in Table 2). The observed planetary atmospheric metallicity-mass trend in our solar system has motivated a number of studies (Thorngren et al. 2016; Welbanks et al. 2019b). As can be seen in Figure 4, our retrieved M/H is within  $1\sigma$  of the trend of methane abundances in the solar system giant planets. Our findings suggest that HD 209458b might have undergone

a similar amount of planetesimal accretion as the solar system giant planets.

The interior model in Thorngren & Fortney (2019) anticipates the maximum metal enrichment for an exoplanet population given its mass and radius for a “core-less” planet (i.e., the metals and gas are thoroughly mixed within the whole planet). These upper limits (as shown with blue circles in Figure 4) greatly exceed the observed Jupiter and Saturn metal enrichments, implying that a huge percentage of metals must be trapped within a core. The atmospheric metallicity of HD 209458b below this limit indicates that some of the accreted metal is also in its core.

The constraint on the atmospheric C/O of HD 209458b from our spectrum is driven by a combination of the detected H<sub>2</sub>O and CO<sub>2</sub>, and the lack of detection of other molecules like CH<sub>4</sub> that would be present in atmospheres with higher C/O values. In Figure 1(b), we show models with C/O = 0.5, 1.0, and 1.5. We find that with a higher C/O ratio, the water feature at  $2.3 \mu\text{m}$  is weakened and the CO<sub>2</sub> feature is enhanced until both of them are absent for C/O > 1. CH<sub>4</sub> takes up the high carbon abundance above C/O ratios of unity.

The low C/O ratio for HD 209458b inferred in our work is due to the strong H<sub>2</sub>O absorption feature, which indicates a high oxygen abundance. As a comparison, we plotted the *JWST* transmission spectra in units of scale height for WASP-39b and HD 209458b in Figure 5 (left). HD 209458b exhibits a relatively stronger H<sub>2</sub>O feature and a weaker CO<sub>2</sub> feature in comparison to WASP-39b. The latter exoplanet has a C/O ranging from 0.3 to 0.46, as reported in the NIR-Spec G395H paper (Alderson et al. 2023). The C/O from this particular paper is chosen due to its bandpass similarity to our work. In Figure 5 (right), we show the ratio of H<sub>2</sub>O and CO<sub>2</sub> abundances as a function of C/O ratio expected from chemical equilibrium. The  $\chi_{\text{H}_2\text{O}}/\chi_{\text{CO}_2}$  has



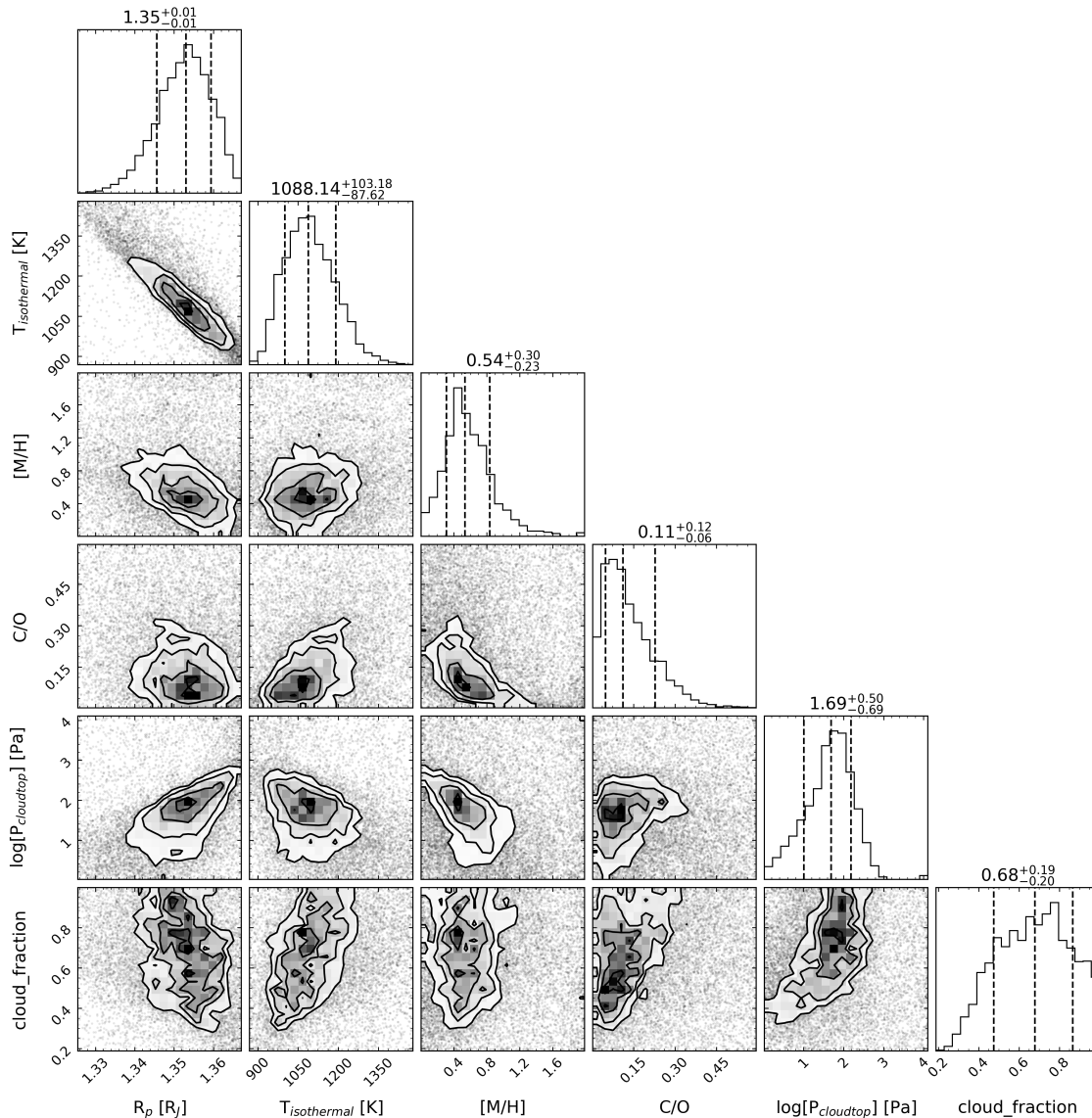


**Figure 3.** Corner plot of the equilibrium chemistry retrieval.

a dependence on metallicity because  $\text{CO}_2$  itself is a strong function of metallicity. Nevertheless, given the similar metallicities of the two planets (WASP-39b is  $\sim 10 \times$  solar, [JTEC ERS Team et al. 2023](#)), the  $\chi_{\text{H}_2\text{O}}/\chi_{\text{CO}_2}$  ratio is mostly indicative of the different C/O ratios of the planets. The relative strength of  $\text{H}_2\text{O}$  vs.  $\text{CO}_2$  absorption thus demonstrates that HD 209458b’s C/O ratio is significantly lower than that of WASP-39b.

In addition to the main atmospheric retrieval described above, we performed a grid fit using the ScCHIMERA Radiative Convective Equi-

librium (RCE) solver first described in [Piskorz et al. \(2018\)](#) and recently used in JWST observations of WASP-39b ([Rustamkulov et al. 2023](#)), WASP-96b ([Radica et al. 2023](#)), and WASP-80b ([Bell et al. 2023](#)). We computed a grid of models under the assumption of 1-dimensional RCE given an irradiation and elemental composition. The grid is computed for steps in the irradiation temperature of  $T_{\text{irr}}$  (1347 – 1557 K in steps of 15 K),  $[\text{M}/\text{H}]$  (-0.5 – 2.25 in steps of 0.125), and C/O (0.1 – 0.75 in steps of 0.05). A detailed description of the ScCHIMERA grid and parameter estimation is

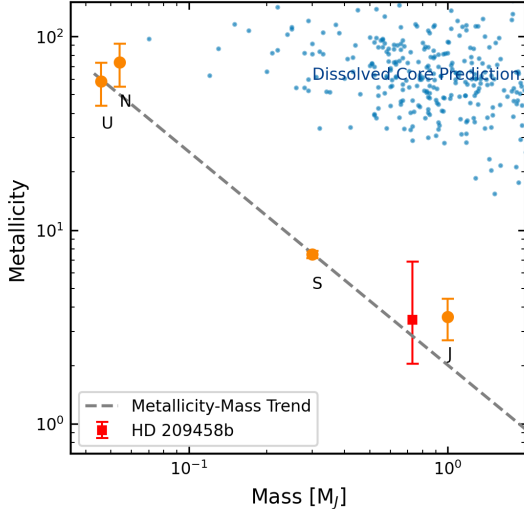


**Figure 4.** Atmospheric metallicity - planet mass trend. Grey dashed line shows metallicity-mass trend linearly regressed by  $(M/H)$  relative to solar =  $A \times \log(\text{Mass}) + B$ . The solar system giant planet data adapted from Thorngren et al. (2016) with the carbon abundance adopted as a proxy for the overall metallicity. The blue circles are obtained from Thorngren & Fortney (2019) showing a planet without a core with all metals uniformly mixed throughout the gas.

available in Radica et al. (2023) and Bell et al. (2023).

Generally, we performed the parameter estimation over the ScCHIMERA grid by post-processing the 1D-RCE atmospheric structures through a transmission spectrum routine while considering the presence of inhomogeneous clouds and power-law hazes. The resulting parameter estimation derived a metallicity of  $\sim 1 - 2 \times$  solar and a sub-solar C/O ratio. The C/O ratio runs up against the lower bound limit of the grid (0.1) and has a  $2\sigma$  upper limit of 0.32. Given the consistency of the results from the two different types of retrievals we emphasize the PLATON results as the main finding in this paper.

Kawashima & Min (2021) report large differences in  $\text{CH}_4$  abundance and C/O between equilibrium and disequilibrium limits when retriev-

ing spectra covering  $2.5 - 4.0 \mu\text{m}$ . By introducing eddy diffusion transport, they found  $\text{CH}_4$  quenches at  $P = 1$  bar thus resulting in less  $\text{CH}_4$  compared to the equilibrium case and C/O is raised to 0.5 in disequilibrium as compared to 0.19 in equilibrium. In order to test the impact of chemical disequilibrium on C/O, on top of the six parameters discussed in §3, we added one more free parameter `P_quenching` in PLATON, the pressure at which quenching happens. However, `P_quenching` cannot be constrained according to our retrieval. Though our results disfavor the disequilibrium scenario, this may partly be because we assume the same quenching pressure for all molecules, while in reality it should be different (Moses 2014). We also assume an isothermal atmosphere with fixed abundance profile while in Kawashima & Min (2021) the profile varies within the retrieval. Further modeling work on this data set using more sophisticated treatments of disequilibrium chemistry are thus warranted.

## 5. DISCUSSION

In this paper, we present the transmission spectrum of the transiting hot Jupiter HD 209458b with data observed with *JWST*/NIRCam from  $2.3 - 5.1 \mu\text{m}$ . The data show clear features from water, carbon dioxide, and clouds. We do not detect evidence for additional molecules that had been previously claimed for this planet. Our retrieval results suggest a mild atmospheric metallicity enhancement between that of Jupiter and Saturn in our own solar system. The data also suggest a very low C/O ratio that stands out from other emerging *JWST* results for giant exoplanets.

In terms of non-detections, our upper limits on the abundances of  $\text{CH}_4$ , HCN, and  $\text{C}_2\text{H}_2$  in particular make the presence of these molecules in the atmosphere of HD 209458b as claimed by Hawker et al. (2018, HCN only) and Giacobbe et al. (2021, all three molecules) controversial.

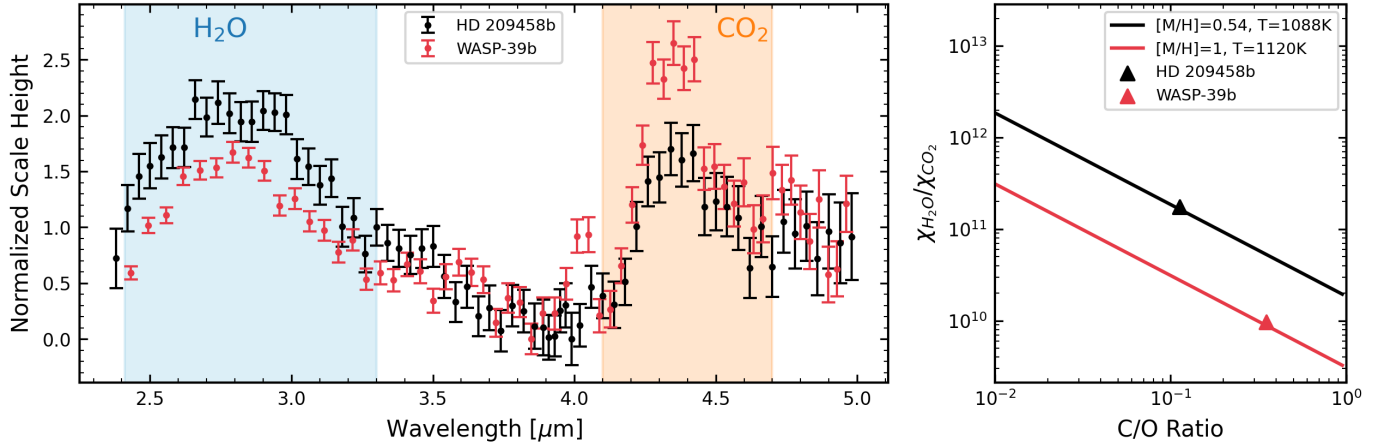


**Figure 5.** Left: *JWST* transmission spectra of HD 209458b and WASP-39b (spectrum adopted from Rustamkulov et al. 2023)) normalized by their atmospheric scale heights. Right: Calculated ratio of water and carbon dioxide abundance as a function of C/O at  $P = 1$  mbar for the retrieved metallicity and temperature of each planet, calculated under the assumption of equilibrium chemistry. The triangle points show the abundance ratio based on their retrieved C/O. As can be seen from the spectra, HD 209458b has a higher ratio of H<sub>2</sub>O to CO<sub>2</sub> abundances, thus implying that it has a lower C/O ratio.

Nevertheless, it is important to point out that Giacobbe et al. (2021) did not perform a retrieval to put formal constraints on the abundances of the molecules they detected due to the challenge of such analyses on HRS data (e.g., Brogi & Line 2019). Therefore, it is not clear what the statistical significance is of the possible tension between the results. HRS in principle may be sensitive to trace species that elude low-resolution spectroscopy, but it remains to be seen whether the very low abundances constrained by our data would still yield a detection in HRS data.

Studies on the robustness of molecular detections by HRS of exoplanets demonstrate that some detrending methods may induce false positive or inflated detections (Cheverall et al. 2023). In their case study on HD 209458b, HCN, NH<sub>3</sub> and CH<sub>4</sub> were not observed by Cheverall et al. (2023). However, a signal for CH<sub>4</sub> can be detected if the telluric contamination is not correctly removed. While methane (CH<sub>4</sub>) is ubiquitous in the atmosphere of solar system giant planets, its absence has long been one of the core puzzles of the study of exoplanetary

atmospheres (Gibson et al. 2011; Benneke et al. 2019; Baxter et al. 2021; JTEC ERS Team et al. 2023). However, recent *JWST* observations on transiting exoplanets WASP-80 b and K2-18 b show evidence of methane (Bell et al. 2023; Madhusudhan et al. 2023). Understanding this molecule’s absence or existence is essential for understanding how planets form and evolve, how atmospheric processes work, and the habitability of planets. Future *JWST* observations, like cycle 2 program 3557, might aid in solving this mystery.

Our study disproves the previous claims of low water abundance for this planet (Madhusudhan et al. 2014; MacDonald & Madhusudhan 2017a; Brogi et al. 2017; Welbanks et al. 2019a; Pinhas et al. 2019). Instead of being depleted in water, our best-fit model gives enhanced metallicity and low C/O, indicating the atmosphere of HD 209458b is rich in oxygen. We found a metallicity that is consistent with, but more precise than Line et al. (2016) in emission and Welbanks & Madhusudhan (2021) in transmission, which extends the agreement that is seen

between the solar system trend and exoplanet atmosphere abundances.

Line et al. (2016) and Brogi et al. (2017) have constrained the C/O of HD 209458b to  $< 1$ , yet our very low C/O ratio provides valuable insights into the planetary formation and evolution. Espinoza et al. (2017) suggests a low C/O in gas giants compared to parent stars is caused by metal enrichment but not dependent on the formation location. Additionally, planetesimal pollution (Öberg et al. 2011) caused by formation and migration sufficiently inward of the snowlines of carbon-bearing species may also result in low ( $< 0.5$ ) C/O and elevated metal enrichment. Through a comparative analysis of the spectra of this study and WASP-39b, we found the two have similar molecular features (namely water and CO<sub>2</sub>), while the variation in the ratio of water to carbon dioxide abundance leads to a distinct difference in the C/O. This is primarily because the value of  $\chi_{\text{H}_2\text{O}}/\chi_{\text{CO}_2}$  serves as a robust indicator of C/O, assuming comparable metallicity. It is important to note that this relationship is not influenced by specific retrieval models, thus revealing the intrinsic characteristics of such planets.

Tsai et al. (2023) showed evidence of photochemically-produced SO<sub>2</sub> in the atmosphere of WASP-39b. Since we do not detect SO<sub>2</sub> at 4.05  $\mu\text{m}$ , we have not made an effort to study the potential impact of chemical disequilibrium on the H<sub>2</sub>S and SO<sub>2</sub> abundance. Detailed modeling to assess our JWST transmission spectrum in the context of the disequilibrium process would be interesting.

## 6. DATA AVAILABILITY

The data presented in this paper were obtained from the Mikulski Archive for Space Telescopes (MAST) at the Space Telescope Science Institute. The specific observations analyzed can be accessed via DOI: [10.17909/f5j3-jq48](https://doi.org/10.17909/f5j3-jq48). The data that were used to create all of the figures will be freely available on Zenodo (Xue

et al. 2024). All additional data is available upon request.

## 7. ACKNOWLEDGMENTS

We thank Matteo Brogi for helpful discussions about the high-resolution spectroscopy results for HD 209458b. This work is based on observations made with the NASA/ESA/CSA James Webb Space Telescope. The data were obtained from the Mikulski Archive for Space Telescopes at the Space Telescope Science Institute, which is operated by the Association of Universities for Research in Astronomy, Inc., under NASA contract NAS 5-03127 for JWST. These observations are associated with program GTO 1274.

This publication makes use of The Data & Analysis Center for Exoplanets (DACE), which is a facility based at the University of Geneva (CH) dedicated to extrasolar planets data visualisation, exchange and analysis. DACE is a platform of the Swiss National Centre of Competence in Research (NCCR) PlanetS, federating the Swiss expertise in Exoplanet research. The DACE platform is available at <https://dace.unige.ch>.

*Facilities:* JWST(NIRCam)

*Software:* Eureka! (Bell et al. 2022), PLATON (Zhang et al. 2020), SPARTA (Kempton et al. 2023), Astropy (Astropy Collaboration et al. 2013, 2018, 2022), dynesty (Speagle 2020), batman (Kreidberg 2015), hitran (Gordon et al. 2022), HELIOSK (Grimm et al. 2021), Fastchem (Stock et al. 2018)

## APPENDIX

## REFERENCES

- Ahrer, E., Wheatley, P. J., Kirk, J., et al. 2022, Monthly Notices of the Royal Astronomical Society, 510, 4857, doi: [10.1093/mnras/stab3805](https://doi.org/10.1093/mnras/stab3805)
- Ahrer, E.-M., Stevenson, K. B., Mansfield, M., et al. 2023, Nature, 614, 653, doi: [10.1038/s41586-022-05590-4](https://doi.org/10.1038/s41586-022-05590-4)
- Alderson, L., Wakeford, H. R., Alam, M. K., et al. 2023, Nature, 614, 664, doi: [10.1038/s41586-022-05591-3](https://doi.org/10.1038/s41586-022-05591-3)
- Asplund, M., Amarsi, A. M., & Grevesse, N. 2021, A&A, 653, A141, doi: [10.1051/0004-6361/202140445](https://doi.org/10.1051/0004-6361/202140445)



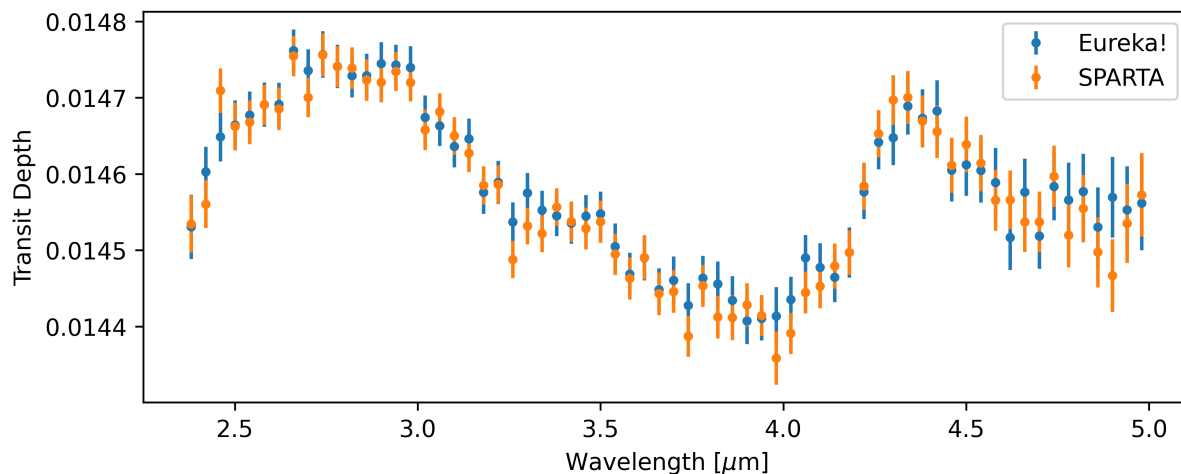


**Figure 6.** Spectra reduced by Eureka! and SPARTA. The data behind the figure can be found in §6.

- Astropy Collaboration, Robitaille, T. P., Tollerud, E. J., et al. 2013, *A&A*, 558, A33, doi: [10.1051/0004-6361/201322068](https://doi.org/10.1051/0004-6361/201322068)
- Astropy Collaboration, Price-Whelan, A. M., Sipőcz, B. M., et al. 2018, *AJ*, 156, 123, doi: [10.3847/1538-3881/aabc4f](https://doi.org/10.3847/1538-3881/aabc4f)
- Astropy Collaboration, Price-Whelan, A. M., Lim, P. L., et al. 2022, *ApJ*, 935, 167, doi: [10.3847/1538-4357/ac7c74](https://doi.org/10.3847/1538-4357/ac7c74)
- August, P. C., Bean, J. L., Zhang, M., et al. 2023, *ApJL*, 953, L24, doi: [10.3847/2041-8213/ace828](https://doi.org/10.3847/2041-8213/ace828)
- Baxter, C., Désert, J.-M., Tsai, S.-M., et al. 2021, *A&A*, 648, A127, doi: [10.1051/0004-6361/202039708](https://doi.org/10.1051/0004-6361/202039708)
- Bean, J. L., Xue, Q., August, P. C., et al. 2023, *Nature*, doi: [10.1038/s41586-023-05984-y](https://doi.org/10.1038/s41586-023-05984-y)
- Bell, T. J., Ahrer, E.-M., Brande, J., et al. 2022, doi: [10.48550/ARXIV.2207.03585](https://doi.org/10.48550/ARXIV.2207.03585)
- Bell, T. J., Welbanks, L., Schlawin, E., et al. 2023, Methane Throughout the Atmosphere of the Warm Exoplanet WASP-80b. <https://arxiv.org/abs/2309.04042>
- Benneke, B., & Seager, S. 2012, *ApJ*, 753, 100, doi: [10.1088/0004-637X/753/2/100](https://doi.org/10.1088/0004-637X/753/2/100)
- Benneke, B., Knutson, H. A., Lothringer, J., et al. 2019, *Nature Astronomy*, 3, 813, doi: [10.1038/s41550-019-0800-5](https://doi.org/10.1038/s41550-019-0800-5)
- Booth, R. A., Clarke, C. J., Madhusudhan, N., & Ilee, J. D. 2017, *MNRAS*, 469, 3994, doi: [10.1093/mnras/stx1103](https://doi.org/10.1093/mnras/stx1103)
- Brogi, M., Line, M., Bean, J., Désert, J.-M., & Schwarz, H. 2017, *The Astrophysical Journal*, 839, L2, doi: [10.3847/2041-8213/aa6933](https://doi.org/10.3847/2041-8213/aa6933)
- Brogi, M., & Line, M. R. 2019, *AJ*, 157, 114, doi: [10.3847/1538-3881/aaffd3](https://doi.org/10.3847/1538-3881/aaffd3)
- Burrows, A., Hubeny, I., Budaj, J., Knutson, H. A., & Charbonneau, D. 2007, *The Astrophysical Journal*, 668, L171, doi: [10.1086/522834](https://doi.org/10.1086/522834)
- Charbonneau, D., Brown, T. M., Latham, D. W., & Mayor, M. 2000, *The Astrophysical Journal*, 529, L45, doi: [10.1086/312457](https://doi.org/10.1086/312457)
- Charbonneau, D., Brown, T. M., Noyes, R. W., & Gilliland, R. L. 2002, *The Astrophysical Journal*, 568, 377, doi: [10.1086/338770](https://doi.org/10.1086/338770)
- Cheverall, C. J., Madhusudhan, N., & Holmberg, M. 2023, Robustness Measures for Molecular Detections using High-Resolution Transmission Spectroscopy of Exoplanets, arXiv. <http://arxiv.org/abs/2303.01496>
- Constantinou, S., Madhusudhan, N., & Gandhi, S. 2023, Early Insights for Atmospheric Retrievals of Exoplanets using JWST Transit Spectroscopy, arXiv. <http://arxiv.org/abs/2301.02564>
- Coulombe, L.-P., Benneke, B., Challener, R., et al. 2023, *Nature*, 620, 292, doi: [10.1038/s41586-023-06230-1](https://doi.org/10.1038/s41586-023-06230-1)
- Deming, D., Seager, S., Richardson, L. J., & Harrington, J. 2005, *Nature*, 434, 740, doi: [10.1038/nature03507](https://doi.org/10.1038/nature03507)
- Deming, D., Wilkins, A., McCullough, P., et al. 2013a, *The Astrophysical Journal*, 774, 95, doi: [10.1088/0004-637X/774/2/95](https://doi.org/10.1088/0004-637X/774/2/95)

- . 2013b, *The Astrophysical Journal*, 774, 95, doi: [10.1088/0004-637X/774/2/95](https://doi.org/10.1088/0004-637X/774/2/95)
- Diamond-Lowe, H., Stevenson, K. B., Bean, J. L., Line, M. R., & Fortney, J. J. 2014, *The Astrophysical Journal*, 796, 66, doi: [10.1088/0004-637X/796/1/66](https://doi.org/10.1088/0004-637X/796/1/66)
- Espinoza, N., Fortney, J. J., Miguel, Y., Thorngren, D., & Murray-Clay, R. 2017, *ApJL*, 838, L9, doi: [10.3847/2041-8213/aa65ca](https://doi.org/10.3847/2041-8213/aa65ca)
- Feinstein, A. D., Radica, M., Welbanks, L., et al. 2023, *Nature*, 614, 670, doi: [10.1038/s41586-022-05674-1](https://doi.org/10.1038/s41586-022-05674-1)
- Giacobbe, P., Brogi, M., Gandhi, S., et al. 2021, *Nature*, 592, 205, doi: [10.1038/s41586-021-03381-x](https://doi.org/10.1038/s41586-021-03381-x)
- Gibson, N. P., Pont, F., & Aigrain, S. 2011, *Monthly Notices of the Royal Astronomical Society*, 411, 2199, doi: [10.1111/j.1365-2966.2010.17837.x](https://doi.org/10.1111/j.1365-2966.2010.17837.x)
- Gordon, I., Rothman, L., Hargreaves, R., et al. 2022, *Journal of Quantitative Spectroscopy and Radiative Transfer*, 277, 107949, doi: <https://doi.org/10.1016/j.jqsrt.2021.107949>
- Greene, T. P., Kelly, D. M., Stansberry, J., et al. 2017, *Journal of Astronomical Telescopes, Instruments, and Systems*, 3, 035001, doi: [10.1117/1.JATIS.3.3.035001](https://doi.org/10.1117/1.JATIS.3.3.035001)
- Grimm, S. L., Malik, M., Kitzmann, D., et al. 2021, *ApJS*, 253, 30, doi: [10.3847/1538-4365/abd773](https://doi.org/10.3847/1538-4365/abd773)
- Hawker, G. A., Madhusudhan, N., Cabot, S. H. C., & Gandhi, S. 2018, *The Astrophysical Journal*, 863, L11, doi: [10.3847/2041-8213/aac49d](https://doi.org/10.3847/2041-8213/aac49d)
- Hayek, W., Sing, D., Pont, F., & Asplund, M. 2012, *Astronomy & Astrophysics*, 539, A102. <http://www.aanda.org/10.1051/0004-6361/201117868>
- Henry, G. W., Marcy, G. W., Butler, R. P., & Vogt, S. S. 2000, *The Astrophysical Journal*, 529, L41, doi: [10.1086/312458](https://doi.org/10.1086/312458)
- Higson, E., Handley, W., Hobson, M., & Lasenby, A. 2018, *Statistics and Computing*, 29, 891, doi: [10.1007/s11222-018-9844-0](https://doi.org/10.1007/s11222-018-9844-0)
- Horne, K. 1986, *Publications of the Astronomical Society of the Pacific*, 98, 609, doi: [10.1086/131801](https://doi.org/10.1086/131801)
- Jiang, C., Chen, G., Palle, E., et al. 2021, *Astronomy & Astrophysics*, 656, A114, doi: [10.1051/0004-6361/202141824](https://doi.org/10.1051/0004-6361/202141824)
- JTEC ERS Team, Ahrer, E.-M., Alderson, L., et al. 2023, *Nature*, 614, 649, doi: [10.1038/s41586-022-05269-w](https://doi.org/10.1038/s41586-022-05269-w)
- Kawashima, Y., & Min, M. 2021, *Astronomy & Astrophysics*, 656, A90, doi: [10.1051/0004-6361/202141548](https://doi.org/10.1051/0004-6361/202141548)
- Kempton, E. M. R., Bean, J. L., Louie, D. R., et al. 2018, *PASP*, 130, 114401, doi: [10.1088/1538-3873/aadf6f](https://doi.org/10.1088/1538-3873/aadf6f)
- Kempton, E. M.-R., Zhang, M., Bean, J. L., et al. 2023, *Nature*, doi: [10.1038/s41586-023-06159-5](https://doi.org/10.1038/s41586-023-06159-5)
- Kipping, D. M. 2013, *Monthly Notices of the Royal Astronomical Society*, 435, 2152, doi: [10.1093/mnras/stt1435](https://doi.org/10.1093/mnras/stt1435)
- Knutson, H. A., Charbonneau, D., Allen, L. E., Burrows, A., & Megeath, S. T. 2008, *The Astrophysical Journal*, 673, 526, doi: [10.1086/523894](https://doi.org/10.1086/523894)
- Kreidberg, L. 2015, *Publications of the Astronomical Society of the Pacific*, 127, 1161, doi: [10.1086/683602](https://doi.org/10.1086/683602)
- Line, M. R., & Parmentier, V. 2016, *ApJ*, 820, 78, doi: [10.3847/0004-637X/820/1/78](https://doi.org/10.3847/0004-637X/820/1/78)
- Line, M. R., Stevenson, K. B., Bean, J., et al. 2016, *The Astronomical Journal*, 152, 203, doi: [10.3847/0004-6256/152/6/203](https://doi.org/10.3847/0004-6256/152/6/203)
- MacDonald, R. J., & Madhusudhan, N. 2017a, *Monthly Notices of the Royal Astronomical Society*, 469, 1979, doi: [10.1093/mnras/stx804](https://doi.org/10.1093/mnras/stx804)
- . 2017b, *The Astrophysical Journal*, 850, L15, doi: [10.3847/2041-8213/aa97d4](https://doi.org/10.3847/2041-8213/aa97d4)
- Madhusudhan, N., Crouzet, N., McCullough, P. R., Deming, D., & Hedges, C. 2014, *The Astrophysical Journal*, 791, L9, doi: [10.1088/2041-8205/791/1/L9](https://doi.org/10.1088/2041-8205/791/1/L9)
- Madhusudhan, N., Sarkar, S., Constantinou, S., et al. 2023, *Carbon-bearing Molecules in a Possible Hycean Atmosphere*. <https://arxiv.org/abs/2309.05566>
- Moses, J. I. 2014, *Philosophical Transactions of the Royal Society A: Mathematical, Physical and Engineering Sciences*, 372, 20130073, doi: [10.1098/rsta.2013.0073](https://doi.org/10.1098/rsta.2013.0073)
- Mousis, O., Lunine, J. I., Madhusudhan, N., & Johnson, T. V. 2012, *ApJL*, 751, L7, doi: [10.1088/2041-8205/751/1/L7](https://doi.org/10.1088/2041-8205/751/1/L7)
- Owen, T., & Encrenaz, T. 2006, *Planet. Space Sci.*, 54, 1188, doi: [10.1016/j.pss.2006.05.030](https://doi.org/10.1016/j.pss.2006.05.030)

- Pinhas, A., Madhusudhan, N., Gandhi, S., & MacDonald, R. J. 2019, *Monthly Notices of the Royal Astronomical Society*, 482, 1485, doi: [10.1093/mnras/sty2544](https://doi.org/10.1093/mnras/sty2544)
- Piskorz, D., Buzard, C., Line, M. R., et al. 2018, *AJ*, 156, 133, doi: [10.3847/1538-3881/aad781](https://doi.org/10.3847/1538-3881/aad781)
- Radica, M., Welbanks, L., Espinoza, N., et al. 2023, *MNRAS*, 524, 835, doi: [10.1093/mnras/stad1762](https://doi.org/10.1093/mnras/stad1762)
- Rustamkulov, Z., Sing, D. K., Mukherjee, S., et al. 2023, *Nature*, 614, 659, doi: [10.1038/s41586-022-05677-y](https://doi.org/10.1038/s41586-022-05677-y)
- Schwarz, H., Brogi, M., de Kok, R., Birkby, J., & Snellen, I. 2015, *Astronomy & Astrophysics*, 576, A111, doi: [10.1051/0004-6361/201425170](https://doi.org/10.1051/0004-6361/201425170)
- Sing, D. K., Fortney, J. J., Nikolov, N., et al. 2016, *Nature*, 529, 59, doi: [10.1038/nature16068](https://doi.org/10.1038/nature16068)
- Snellen, I. A. G., de Kok, R. J., de Mooij, E. J. W., & Albrecht, S. 2010, *Nature*, 465, 1049, doi: [10.1038/nature09111](https://doi.org/10.1038/nature09111)
- Speagle, J. S. 2020, *Monthly Notices of the Royal Astronomical Society*, 493, 3132, doi: [10.1093/mnras/staa278](https://doi.org/10.1093/mnras/staa278)
- Spyratos, P., Nikolov, N. K., Constantinou, S., et al. 2023, *Monthly Notices of the Royal Astronomical Society*, 521, 2163, doi: [10.1093/mnras/stad637](https://doi.org/10.1093/mnras/stad637)
- Stassun, K. G., Collins, K. A., & Gaudi, B. S. 2017, *The Astronomical Journal*, 153, 136, doi: [10.3847/1538-3881/aa5df3](https://doi.org/10.3847/1538-3881/aa5df3)
- Stock, J. W., Kitzmann, D., Patzer, A. B. C., & Sedlmayr, E. 2018, *Monthly Notices of the Royal Astronomical Society*, doi: [10.1093/mnras/sty1531](https://doi.org/10.1093/mnras/sty1531)
- Thorngren, D., & Fortney, J. J. 2019, *The Astrophysical Journal*, 874, L31, doi: [10.3847/2041-8213/ab1137](https://doi.org/10.3847/2041-8213/ab1137)
- Thorngren, D. P., Fortney, J. J., Murray-Clay, R. A., & Lopez, E. D. 2016, *The Astrophysical Journal*, 831, 64, doi: [10.3847/0004-637X/831/1/64](https://doi.org/10.3847/0004-637X/831/1/64)
- Tsai, S.-M., Lee, E. K. H., Powell, D., et al. 2023, *Nature*, 617, 483, doi: [10.1038/s41586-023-05902-2](https://doi.org/10.1038/s41586-023-05902-2)
- Tsiaras, A., Waldmann, I. P., Zingales, T., et al. 2018, *The Astronomical Journal*, 155, 156, doi: [10.3847/1538-3881/aaaf75](https://doi.org/10.3847/1538-3881/aaaf75)
- Vidal-Madjar, A., des Etangs, A. L., Désert, J.-M., et al. 2003, *Nature*, 422, 143, doi: [10.1038/nature01448](https://doi.org/10.1038/nature01448)
- Vidal-Madjar, A., Désert, J.-M., Etangs, A. L. d., et al. 2004, *The Astrophysical Journal*, 604, L69, doi: [10.1086/383347](https://doi.org/10.1086/383347)
- Welbanks, L., & Madhusudhan, N. 2021, *ApJ*, 913, 114, doi: [10.3847/1538-4357/abee94](https://doi.org/10.3847/1538-4357/abee94)
- Welbanks, L., Madhusudhan, N., Allard, N. F., et al. 2019a, *The Astrophysical Journal*, 887, L20, doi: [10.3847/2041-8213/ab5a89](https://doi.org/10.3847/2041-8213/ab5a89)
- . 2019b, *The Astrophysical Journal Letters*, 887, L20, doi: [10.3847/2041-8213/ab5a89](https://doi.org/10.3847/2041-8213/ab5a89)
- Xue, Q., Bean, J., Zhang, M., et al. 2024, *Data and model for 'JWST transmission spectroscopy of HD 209458b: a super-solar metallicity, a very low C/O, and no evidence of CH<sub>4</sub>, HCN, or C<sub>2</sub>H<sub>2</sub>', V2.0*, Zenodo, doi: [10.5281/zenodo.10557924](https://doi.org/10.5281/zenodo.10557924)
- Zhang, M., Chachan, Y., Kempton, E. M.-R., et al. 2020, *The Astrophysical Journal*, 899, 27, doi: [10.3847/1538-4357/aba1e6](https://doi.org/10.3847/1538-4357/aba1e6)
- Zhang, M., Chachan, Y., Kempton, E. M.-R., & Knutson, H. A. 2019, *Publications of the Astronomical Society of the Pacific*, 131, 034501, doi: [10.1088/1538-3873/aaf5ad](https://doi.org/10.1088/1538-3873/aaf5ad)
- Öberg, K. I., & Bergin, E. A. 2016, *The Astrophysical Journal Letters*, 831, L19, doi: [10.3847/2041-8205/831/2/L19](https://doi.org/10.3847/2041-8205/831/2/L19)
- Öberg, K. I., Murray-Clay, R., & Bergin, E. A. 2011, *The Astrophysical Journal*, 743, L16, doi: [10.1088/2041-8205/743/1/L16](https://doi.org/10.1088/2041-8205/743/1/L16)